Neural Development

RESEARCH

Open Access

The development of the adult nervous system in the annelid *Owenia fusiformis*

Allan M. Carrillo-Baltodano[1*], Rory D. Donnellan[1], Elizabeth A. Williams[2], Gáspár Jékely[3,4] and José M. Martín-Durán[1]

Abstract

Background The evolutionary origins of animal nervous systems remain contentious because we still have a limited understanding of neural development in most major animal clades. Annelids — a species-rich group with centralised nervous systems — have played central roles in hypotheses about the origins of animal nervous systems. However, most studies have focused on adults of deeply nested species in the annelid tree. Recently, *Owenia fusiformis* has emerged as an informative species to reconstruct ancestral traits in Annelida, given its phylogenetic position within the sister clade to all remaining annelids.

Methods Combining immunohistochemistry of the conserved neuropeptides FVamide-lir, RYamide-lir, RGWamide-lir and MIP-lir with gene expression, we comprehensively characterise neural development from larva to adulthood in *Owenia fusiformis*.

Results The early larval nervous system comprises a neuropeptide-rich apical organ connected through peripheral nerves to a prototroch ring and the chaetal sac. There are seven sensory neurons in the prototroch. A bilobed brain forms below the apical organ and connects to the ventral nerve cord of the developing juvenile. During metamorphosis, the brain compresses, becoming ring-shaped, and the trunk nervous system develops several longitudinal cords and segmented lateral nerves.

Conclusions Our findings reveal the formation and reorganisation of the nervous system during the life cycle of *O. fusiformis*, an early-branching annelid. Despite its apparent neuroanatomical simplicity, this species has a diverse peptidergic nervous system, exhibiting morphological similarities with other annelids, particularly at the larval stages. Our work supports the importance of neuropeptides in animal nervous systems and highlights how neuropeptides are differentially used throughout development.

Keywords Annelid, Larvae, Neuropeptides, Nervous system

Introduction

Nervous systems encompass all the neurons and their connections in an animal and are used to communicate information along the body to elaborate behavioural and physiological responses in front of internal and external stimuli [1]. Nervous systems are morphologically diverse, from diffuse nets as present in some non-bilaterian animals (e.g., ctenophores and cnidarians) to specialised and centralised systems with an anterior brain and postcephalic longitudinal cords, as in many bilaterians [2, 3]. Yet, how nervous systems evolved remains contentious

*Correspondence:
Allan M. Carrillo-Baltodano
a.carrillo-baltodano@qmul.ac.uk
[1] School of Biological and Behavioural Sciences, Queen Mary University of London, London, UK
[2] Faculty of Health and Life Sciences, University of Exeter, Exeter, UK
[3] Living Systems Institute, University of Exeter, Exeter, UK
[4] Centre for Organismal Studies (COS), University of Heidelberg, Heidelberg, Germany

because developmental information is lacking for many animal groups. Comparative, phylogenetically-guided studies on the specification, differentiation, patterning and architecture of nervous systems in as many different groups as possible [4, 5] are thus crucial to understand better how animal nervous systems originated and diversified [6].

Annelids — a group with a biphasic life cycle, a trochophore-like larva and centralised nervous systems as adults — have been central in understanding the evolution of nervous systems [3, 7–12]. Traditionally, however, most studies have focused on species deeply nested in the annelid tree of life [13, 14], primarily on adults, and to a lesser extent using high-resolution developmental time courses [15–20]. Therefore, studying lineages that branch off earlier in Annelida, such as Oweniidae, Magelonidae and Chaetopteriformia, is essential to reconstruct ancestral traits in neural development for this animal clade [13, 21]. Recent works in these groups [12, 21–26] have suggested that a basiepidermal nervous system with a less organised brain was likely present in the last common annelid ancestor, which is a neuroanatomy that correlates well with their sedentary and tube-dwelling lifestyle [22]. These studies have also indicated a simplification of the brain from larva to adult stages [22, 25, 26]. However, we have previously demonstrated that neurogenesis is not so simple and starts with the formation of the anterior neural system comprising the apical organ and associated neurons in the ciliary band that works as the main locomotory organ in the late embryos and early idiosyncratic mitraria larvae of the oweniid *Owenia fusiformis* [23, 24]. When entering a feeding stage, the mitraria larva undergoes a series of morphological transformations and increases in size [23, 24, 27, 28], concurrent with significant changes in gene regulation and the formation of a juvenile rudiment that broadly corresponds to the future adult trunk [23, 24, 27–29]. However, the use of only a few immunostaining markers has prevented a better understanding of neural development in *O. fusiformis*, particularly during metamorphosis.

In this study, we combine cross-species antibodies against a variety of highly-conserved neuropeptides [30–32] with gene expression analyses of anterior marker genes [9, 33, 34] to characterise the development of the nervous system in *O. fusiformis*, from the larval to the adult stages (Fig. 1). Our findings reveal a transition from a bilateral bilobed brain before metamorphosis that fuses during metamorphosis to give rise to a ring-shaped

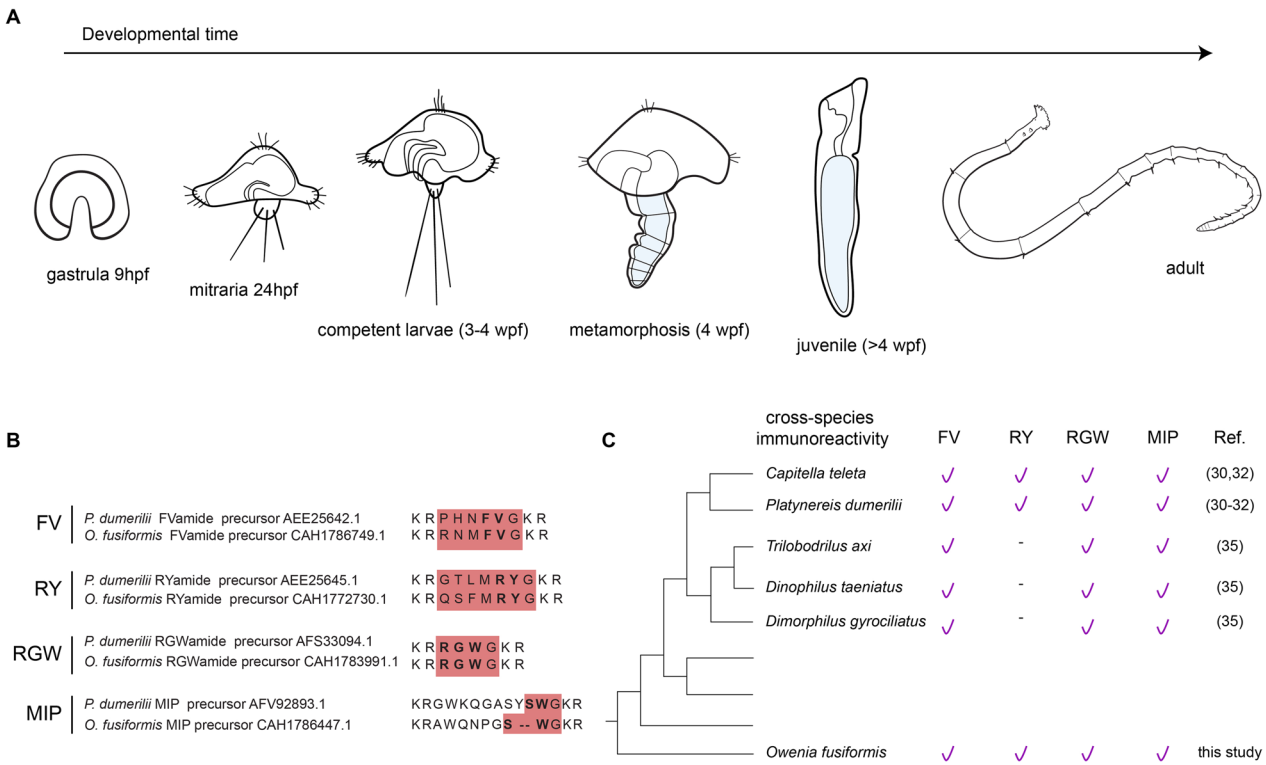

Fig. 1 *Owenia fusiformis* development. **a** Developmental time course of stages studied: gastrula, early larva, competent larva, metamorphosis, juvenile and adult. **b** Conserved motifs in the epitopes of neuropeptides between *Platynereis dumerilii* [30–32] and *Owenia fusiformis*. Representative mature peptides and conserved dipeptides are highlighted in red and bold, respectively. **c** Cross-species reactivity tested across several annelids [31, 32, 35]

brain in the adult. Likewise, it provides new evidence of the brain's connection with the future medullary cord of the trunk and the neural subdivisions in the segmented trunk. Together, we show a previously overlooked level of organisation of the nervous system in *O. fusiformis* that will be important to understanding the early dynamics of neural development in annelids and other animals.

Methods

Animal collection

Reproductive individuals of *O. fusiformis* were collected from the coast near the Station Biologique de Roscoff (France) and kept in the laboratory as previously described [24, 33]. In vitro fertilisation and embryos and larvae cultures were carried out as previously described [24].

Immunohistochemistry

Fixation and antibody staining were conducted as described elsewhere [24]. Adult specimens were relaxed in 8% $MgCl_2$ and fixed overnight at 4 °C with 4% paraformaldehyde in artificial seawater. Adults were then placed in 60 mm dishes in 1x phosphate-buffered saline (PBS), and their heads were dissected with a razor blade between the thoracic and the abdominal segments (between segments three and four [36, 37]). Adult heads were treated post-fixation with 1% collagenase D (Merk-Sigma, # COLLD-RO) overnight at 4 °C and permeabilised through several washes with 1x PBS + 0.5% Triton X-100 (PTx). The primary antibodies mouse anti-acetylated α-tubulin (clone 6-11B-1, Merk-Sigma, #MABT868, 1:800), mouse anti-beta-tubulin (E7, Developmental Studies Hybridoma Bank, 1:20), rabbit anti-FMRFamide (Immunostar, cat#: 20,091, 1:600), and *Platynereis dumerilii* derived [30–32] rabbit anti-FVamide (stock concentration: 0.12 mg/ml; accession number: AEE25642.1, 1:200–1:500), anti-RYamide (stock concentration: 0.28 mg/ml; accession number: AEE25645.1, 1:200–1:500), anti-RGWamide (stock concentration: 0.4 mg/ml; accession number: AFS33094.1, 1:200–1:500) and anti-MIP (myoinhibitory peptide) (stock concentration: 0.28 mg/ml; accession number: AFV92893.1, 1:200–1:500) were diluted in 5% normal goat serum (NGS) in PTx and incubated overnight at 4 °C. After several washes in 1% bovine serum albumin (BSA) in PTx, samples were incubated with AlexaFluor488, AlexaFluor555 and AlexaFluor647 conjugated secondary antibodies (ThermoFisher Scientific, A-21,428, A32731, A-21,235, 1:600) plus DAPI (stock 2 mg/ml, 1:2000) diluted in 5% NGS in PTx overnight at 4 °C. Adults were dehydrated stepwise in isopropanol, cleared in 2:1 benzyl benzoate:benzyl alcohol, briefly immersed in xylene, and mounted in Entellan (Merk-Sigma, #1.07960).

Orthology analysis

A previously published alignment of SOX proteins [38] and maximum likelihood tree reconstruction with FastTree [39] were used to assign the orthology of SOXC in *O. fusiformis*. The orthologies of POU4, SIX3/6, NK2.1, OTX, and ChAt were previously published [9, 33, 34].

Whole-mount in situ hybridisation

Riboprobes were synthesised with the T7 enzyme following the manufacturer's recommendations (Ambion's MEGAscript kit, #AM1334) and stored in hybridisation buffer at a concentration of 50 ng/µl at −20 °C. Single colourimetric in situ hybridisation of embryos and mitraria larvae was performed following an established protocol using a 1.5 ng/µl probe concentration for *soxC*, *pou4*, *six3/6*, *otx*, *nk2.1* and *ChAt* [24, 29, 33, 34].

Imaging

Representative embryos, larvae, and juveniles from the colourimetric whole mount in situ hybridisation experiments were cleared and mounted in 80% glycerol in PBS. They were imaged with a Leica DMRA2 upright microscope equipped with an Infinity5 camera (Lumenera) using differential interference contrast (DIC) optics. Confocal laser scanning microscopy (CLSM) images were taken with a Leica SP5, Leica Stellaris 8 and Nikon CSU-W1 spinning disk confocal microscope. CLSM Z-stack projections were built with ImageJ2 [40] and Nikon NIS-elements software. DIC images were digitally stacked with Helicon Focus 7 (HeliconSoft). Brightness and contrast were edited with Adobe Photoshop CC (v 24.0.0), and figures were built with Adobe Illustrator CC (v 27.0.0) (Adobe Inc.).

Results

To characterise better the complexity and development of the nervous system of *O. fusiformis*, we tested four purified antibodies against conserved mature neuropeptides (FVamide, RYamide, RGWamide and MIP) of the annelid *P. dumerilii* that have broad cross-species immunoreactivity (Figs. 1b–c and 2; Additional file 1: Supplementary Fig. 1; Additional file 2: Supplementary Fig. 2) [30, 32, 35]. FVamide, RYamide and RGWamide label many of the previously described components of the early larval nervous system [24] (Fig. 2), including the apical organ and the prototroch ring, but also previously uncharacterised peripheral nerves in the larval episphere. The MIP antibody has a lower signal-to-noise ratio but still labels the apical organ and some tissue anterior to the larval mouth (Additional file 2: Supplementary Fig. 2). Having confirmed their connection to the larval neural components, we focused on describing the immuno-reactivity

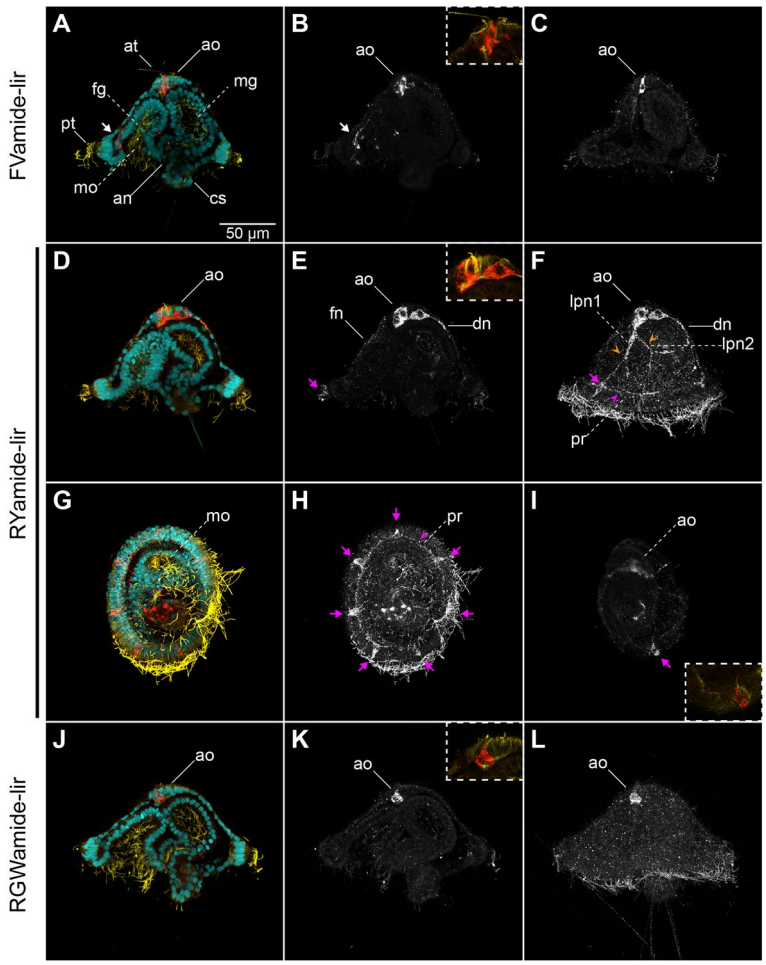

Fig. 2 Neuropeptide-lir elements in the early mitraria. Confocal Laser Scanning Microscopy (CLSM) images of DAPI (cyan), acetylated tubulin (yellow) and neuropeptide-lir (red or white) elements at 24 hpf. All images are lateral views except for ventral views in **g**–**i**. Insets in (**b**, **e**, **i** and **k**) are close ups of the apical organ (ao) in the same view as the larger image. **a**–**c** FVamide-lir cells in the apical organ and one cell anterior to the foregut (white arrow). **d**–**i** RYamide-lir cells are present in the apical organ, with RYamide-lir axons (fn, dn, and orange arrowheads) connecting with seven RYamide-lir cells (magenta arrows) and an RYamide-lir prototrochal ring (pr). **j**–**l** RGWamide-lir cells are exclusively present in the apical organ. an: anus; ao: apical organ; at: apical tuft; cs: chaetal sac; dn: dorsal nerve; fg: foregut; fn: frontal nerve; mg: midgut; mo: mouth; pr: prototrochal ring; pt: prototroch

of these antibodies during the life cycle of *O. fusiformis*, using anti-tubulin as a counter-immunostaining of the nervous system.

The complex nervous system of the early mitraria

At 24 h post-fertilisation (hpf), between three to seven FVamide-like immune-reactive (FVamide-lir), RYamide-lir and RGWamide-lir cells are detectable in the apical organ of the early mitraria larva (Fig. 2). A solitary FVamide-lir neuron with a weak FVamide-lir short axon is positioned anterior and apical to the mouth (white arrow, Fig. 2a–b). MIP has a similar pattern of immunoreactivity (white arrow, Additional file 2: Supplementary Fig. 2). RYamide-lir axons, on the other hand, connect the apical organ to an RYamide-lir prototroch ring (pr) (magenta arrowhead, Fig. 2e–f, h) via a frontal nerve (fn), a dorsal nerve (dn) and two bilateral peripheral nerves (lpn1–2) that bifurcate further midway in the episphere (orange arrowheads, Fig. 2e–f). The prototroch ring also contains seven RYamide-lir cells (magenta arrows, Fig. 2e–f, h–i), three anterior and four posterior, similar to the FMRFamide-lir, *elav*$^{+}$ and *synaptotagmin*$^{+}$ cells previously described at this larval stage [24]. In contrast, RGWamide-lir cells are exclusively restricted to the apical organ (Fig. 2j–l). Apical cilia protrude from some of the FVamide-lir, RYamide-lir, RGWamide-lir and MIP-lir neurons of the apical organ (Fig. 2b, e, j; Additional file 2: Supplementary Fig. 2). At this stage, beta-tubulin

and alpha-acetylated tubulin label the frontal, dorsal, and peripheral nerves connecting the apical organ with the tubulin$^+$ prototroch ring (Fig. 3a–e, h–m). Near the seven refringent globules of unknown function [24, 27], but integrated within the prototroch, are at least five beta-tubulin$^+$ monociliated cells with a short cilium, which likely represent mechanoreceptors (Fig. 3e–g). Together, these new neuropeptide antibodies and more detailed observations of tubulin immunostaining demonstrate the complexity of the apical organ and neural components of the prototroch, including elaborated neurite patterns that connect these two sensorial structures, many of which had been previously overlooked [9, 23, 24].

The formation of the brain and nerve cords

As the larva grows and acquires competence, the adult brain forms, first as a horseshoe-shaped, bilobular, apical condensation of nuclei recognisable, as well, through the cell membrane labelling with beta-tubulin [27] (br; Fig. 4a, e, g, k, m, o, q, u; Additional file 3: Supplementary Fig. 3a, d, g, j; Additional file 4: Supplementary Fig. 4a–d). In addition, the bilateral gene expression of the putative neural gene *soxC* (Additional file 5: Supplementary Fig. 5) and anterior markers *pou4*, *six3/6*, *nk2.1* and *ChAt* (Fig. 5a–f, i–l) confirm the bilobular nature of the brain at this stage. A small pit, as referred to by Wilson [27], is positioned most apically in the brain, where the ciliated

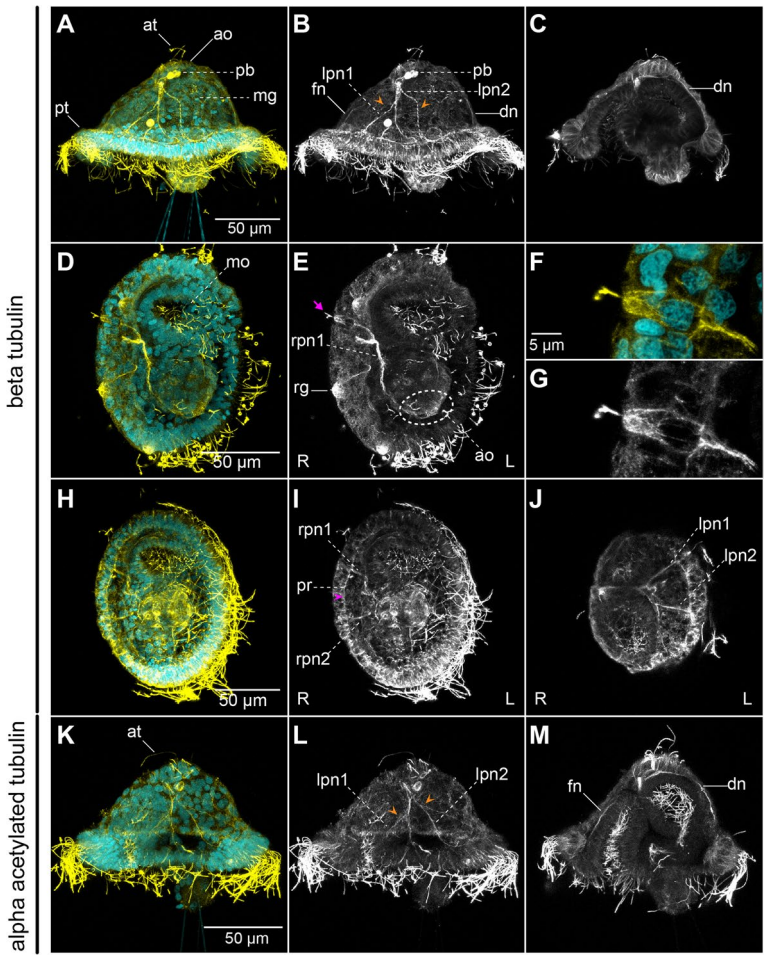

Fig. 3 Tubulin$^+$ elements in the early mitraria. CLSM images of DAPI (cyan) and beta-tubulin (**a**–**j**) and alpha-acetylated tubulin (**k**–**m**) (yellow or white) at 24 hpf. Insets in (**f**–**g**) are close ups of the peripheral neuron in **e**. **a**–**c** Lateral views with beta-tubulin$^+$ axons extending from the apical organ (ao) anteriorly (fn), dorsally (dn) and laterally (rpn, lpn; orange arrowheads) towards the prototroch ring. The polar bodies (pb) are still visible at this stage in the blastocoel space between the apical organ and the midgut (mg). Beta-tubulin is also staining the cell boundaries across the body of the larva, like in **c**. **d**–**g** Ventral views showing at least one beta-tubulin$^+$ monociliated cell (magenta arrow) in the prototroch that presumably connects to the apical organ via a peripheral nerve (rpn1). **h**–**j** Two bilateral peripheral nerves (rpn1–rpn2 and lpn1–lpn2) branch out on each side of the episphere towards the tubulin$^+$ prototrochal ring (pr). **k**–**m** Most of the beta-tubulin$^+$ axons are also with acetylated tubulin. ao: apical organ; at: apical tuft; dn: dorsal nerve; fn: frontal nerve; lpn1–lpn2: left peripheral nerves 1–2; mg: midgut; mo: mouth; pr: prototrochal ring; pt: prototroch; rg: refringent globule; rpn1–rpn2: right peripheral nerves 1–2

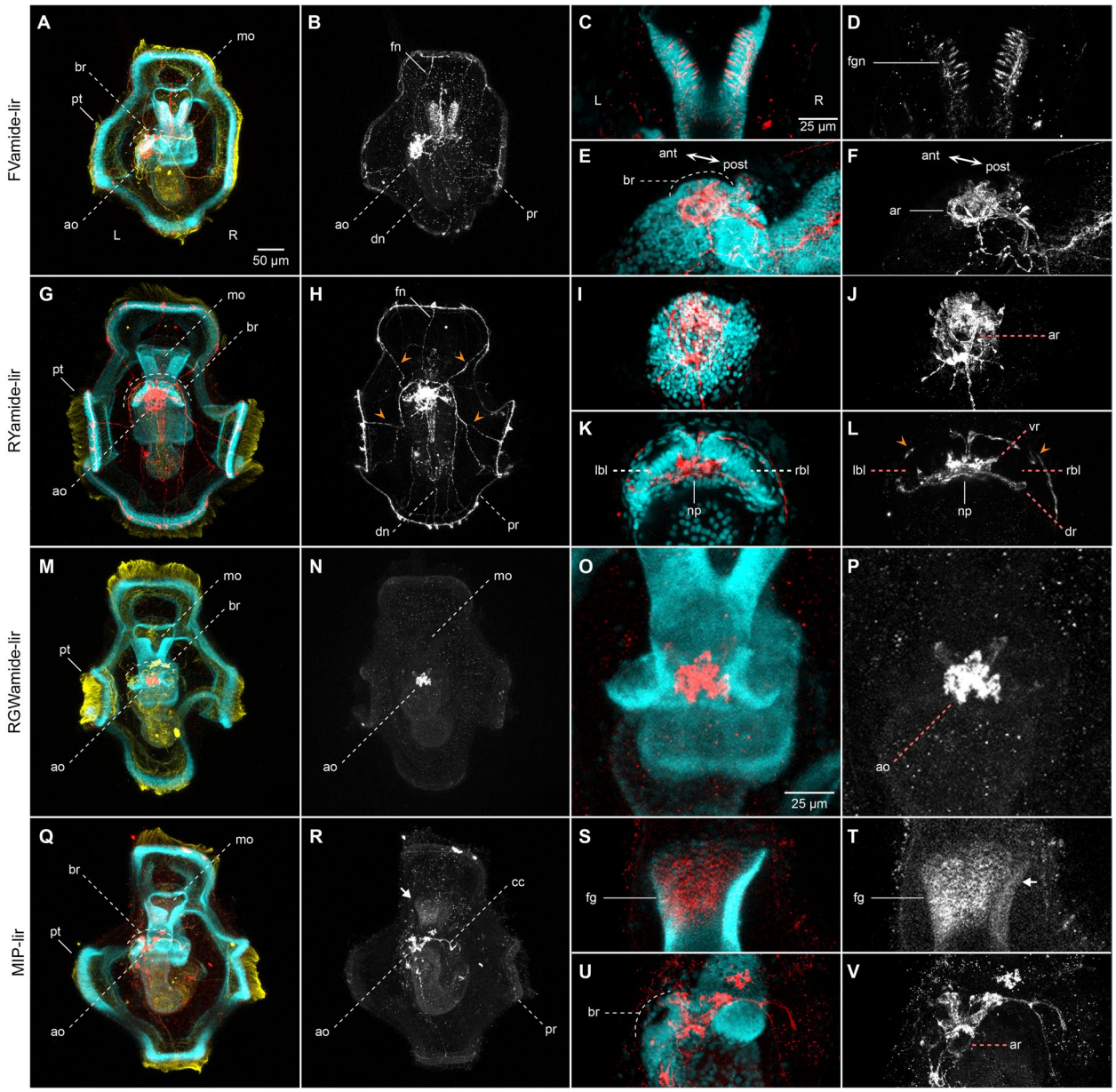

Fig. 4 Neuropeptide-lir elements in the competent larvae. CLSM images of DAPI (cyan), acetylated tubulin (yellow) and neuropeptide-lir (red or white) elements in the competent larvae (~ 3 wpf). Apical views, with anterior to the top. **c**–**f**, **i**–**l**, **o**–**p** and **s**–**v** are close ups of the foregut or apical organ in the same view as the respective larger image in **b**, **h**, **n**, **r**. **a**–**b**, **e**–**f** FVamide-lir cells and **q**–**r**, **u**–**v** MIP-lir cells in the apical organ connect via FVamide-lir and MIP circumesophageal connectives (cc) to the ventral nerve cord (vnc) of the juvenile trunk rudiment (jr) (See Additional file 3: Supplementary Fig. 3), and via **a**–**b** FVamide-lir, **g**–**h** RYamide-lir and **q**–**r** MIP-lir frontal (fn), dorsal (dn) and peripheral nerves (orange arrow heads) to the **a**–**b** FVamide-lir, **g**–**h** RYamide-lir and **q**–**r** MIP-lir prototrochal ring (pr). An **e**–**f** FVamide-lir, **i**–**j** RYamide-lir and **u**–**v** MIP-lir apical nerve ring (ar) surrounds the apical tuft. The foregut is innervated by **a**–**d** FVamide-lir cells and neurites. **k**–**l** RYamide-lir axons form a neuropil between two brain lobes (rbl–lbl) underneath the apical organ. **m**–**p** RGWamide-lir cells remain only in the apical organ. Arrow in **r**, **t** is presumably background staining.an: anus; ao: apical organ; ar: apical nerve ring; at: apical tuft; br: brain; cc: circumesophageal connectives; chn: chaetal sac nerve; cs: chaetal sac; dn: dorsal nerve; dr: dorsal root; fg: foregut; fgn: foregut nerve; fn: frontal nerve; jr: juvenile rudiment; mg: midgut; mo: mouth; np: brain neuropil; pr: prototrochal ring; pt: prototroch; vr: ventral root

apical tuft protrudes (Additional file 4: Supplementary Fig. 4a–b, g–i). In addition, an apical ring of FVamide-lir, RYamide-lir, MIP-lir, and tubulin^{+} cells surround this apical tuft (ar; Fig. 4f, j, v; Additional file 4: Supplementary Fig. 4b, h) and is presumably part of the apical organ. At this stage, this neural larval organ also contains multiple FVamide-lir, RYamide-lir, RGWamide-lir and MIP-lir neurons, interconnected with the brain sitting just below

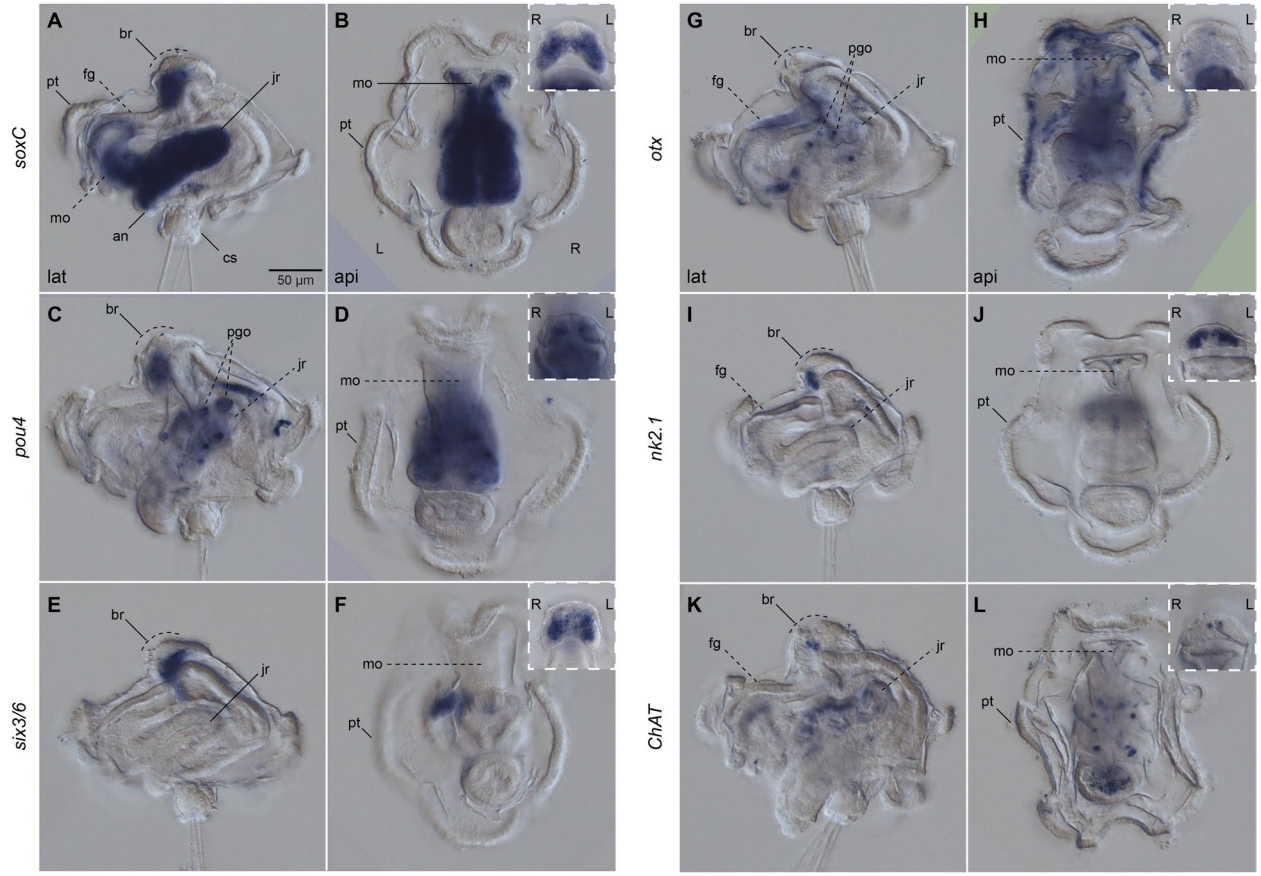

Fig. 5 Expression of neural genes in the competent larvae. Differential Interference Contrast (DIC) images showing expression of *soxC*, *pou4*, *six3/6*, *otx*, *nk2.1* and *ChAt*. **a**, **c**, **e**, **g**, **i**, **k** lateral views; **b**, **d**, **f**, **h**, **j**, **l** apical views. Insets are close ups of the corresponding larger images in anterior view. All genes, except for *otx* **g**–**h**, have a bilateral expression in the brain (br). **a**–**b** *soxC* is strongly expressed in the juvenile rudiment (jr), the mouth (mo), and the anterior part of the foregut (fg). **g**–**l** *otx*, *nk2.1* and *ChAt* have some weaker expression in the foregut. **g**–**h** in addition *otx* is expressed in the prototroch. an: anus; br: brain; cs: chaetal sac; fg: foregut; jr: juvenile rudiment; mo: mouth; pgo: parapodial glandular organ; pt: prototroch

(ao; Fig. 4a–b, d–f, g–l, m–r, u–v; Additional file 3: Supplementary Fig. 3). Two thick RYamide-lir and tubulin$^+$ axon bundles — the ventral and dorsal roots — cross the brain and form a central neuropil just below the condensed nuclei of the brain [23, 27] (Fig. 4k–l; Additional file 4: Supplementary Fig. 4c, h). We used the terms "ventral" root and "dorsal" root to follow the nomenclature of the brain in other annelids [14, 41]. However, the ventral and dorsal roots are positioned anteriorly and posteriorly, respectively, along the main body axis of the larva and juvenile. Altogether, these apical neural structures connect with the developing ventral nerve cord (vnc) of the juvenile rudiment (see below) through FVamide-lir, MIP-lir (Additional file 3: Supplementary Fig. 3b, k), and tubulin$^+$ (Additional file 4: Supplementary Fig. 4b) circumesophageal connectives. Eyespots are present on each side of the most basal part of the brain (not shown) [23, 27]. Lastly, frontal and dorsal nerves, plus the lateral peripheral nerves, maintain the connection between the apical organ/brain and the prototroch neural ring (Fig. 4b, h, r; Additional file 3: Supplementary Fig. 3b, e, k; Additional file 4: Supplementary Fig. 4f, i).

At this pre-metamorphic larval stage, the juvenile rudiment has grown into a defined trunk, with segments that will wrap around the gut as it prepares to evaginate from the larval body [27–29]. The vnc of the trunk starts forming as early as two weeks post fertilisation (wpf) and is immunoreactive to serotonin (5HT), FMRFamide and tubulin [23]. Between two to three wpf, 5HT-lir and FMRFamide-lir neurons and lateral nerves presumably get patterned on each of the developing trunk segments [23]. In agreement with the expression of *elav* and *synaptotagmin*, *soxC* is highly expressed in the juvenile trunk at this stage, supporting that this is a prominent site of active neurogenesis in the competent larva [24] (Fig. 5a–b). Not only has the trunk an FVamide-lir, RYamide-lir, MIP-lir and tubulin$^+$ vnc but also an FVamide-lir and RYamide-lir dorsal one (Additional file 3: Supplementary

Fig. 3c, f), demonstrating that many of the components of the adult peripheral nervous system develop before metamorphosis.

In addition to the developing brain and nerve cords, the foregut is innervated with FVamide-lir and RYamide-lir neurons and nerves (fgn; Fig. 4d, h; Additional file 3: Supplementary Fig. 3b–c, e–f). MIP shows some unspecific labelling at the anterior section of the foregut (Fig. 4s–t; Additional file 3: Supplementary Fig. 3k–l), mirroring the expression domains of *soxC*, *otx*, *nk2.1*, and *ChAt* in this larval region (Fig. 5a, g, i, k). Dorsal to the posterior tip of the trunk, the larval chaetal sac, which has many more chaetae at this stage than in the early mitraria, has an RYamide-lir and MIP-lir nerve connecting these defensive structures to the peripheral neurites of the episphere (Additional file 3: Supplementary Fig. 3f, l). Altogether, the comprehensive analysis of the nervous system of the competent larva of *O. fusiformis* reveals a transition of neural connectivity, where the forming adult brain remains connected to the transitory larval organs, such as the prototroch and chaetal sac, as the connections with the developing trunk nervous system are established.

The nervous system during metamorphosis

The apical organ remains positioned dorsally and apically to the double root of axons of the brain (i.e., the central neuropil; Fig. 6; Additional file 6: Supplementary Fig. 6a), and continues to be connected with the larval episphere and prototroch ring with the FVamide-lir, RYamide-lir and tubulin$^+$ dorsal nerves (Additional file 6: Supplementary Fig. 6a–d; Additional file 7: Supplementary Fig. 7b), and RYamide-lir and tubulin$^+$ lateral nerves (Fig. 6c–d; Additional file 6: Supplementary Fig. 6c–d; Additional file 6: Supplementary Fig. 7a–b). The distinct two lobes of the brain of the competent larva appear to fuse into a continuous horseshoe shape during metamorphosis (Fig. 7b, f), forming the putative ring-shaped brain of the juvenile and adult (see below). The dorsal and ventral root of the brain creates an FVamide-lir, RYamide-lir, RGWamide-lir, MIP-lir and tubulin$^+$ neuropil (np; Fig. 6c, f, i, l; Additional file 7: Supplementary Fig. 7a–b), which connects to the thorax of the evaginating trunk via circumesophageal connectives (or lateral medullary cords [22]; see discussion) (Fig. 6; Additional file 6: Supplementary Fig. 6; Additional file 7: Supplementary Fig. 7a–b). In the juvenile and adult, the thorax is composed of three fused trunk segments, which we name ciliated thoracic segments (cts), and differentiate from the other trunk segments by having capillary chaetae [36, 37] and abundant cilia in the epidermis (Additional file 7: Supplementary Fig. 7a–b). Paired RGWamide-lir parapodial glandular organs (pgos) up to the seventh segment [27, 42] facilitate the distinction between the three thoracic and the seven abdominal segments [27, 28] (Fig. 6g–h; Additional file 6: Supplementary Fig. 6e–f). We could not observe ganglia in either thoracic or abdominal segments using nuclear staining and gene expression (Fig. 7), providing further evidence of the medullary cord nature in oweniids [12, 22]. However, several iterated FVamide-lir, RYamide-lir, RGWamide-lir, and MIP-lir neurons are present along the vnc, which are more condensed in the thorax because of the fusion of the three thoracic segments and more distant in the rest of the trunk (Fig. 6a–b, d–e, g–h, j–k; Additional file 6: Supplementary Fig. 6). From these clusters of iterated neurons, FVamide-lir, RYamide-lir, RGWamide-lir, MIP-lir and tubulin$^+$ lateral nerves run on the anterior edge of each segment transversally towards the dorsal side of the trunk, connecting to the dorsal nerve cord (Additional file 6: Supplementary Fig. 6; Additional file 7: Supplementary Fig. 7b). During metamorphosis, the foregut will break from the larval tissue to connect with the brain and become the definite mouth of the juvenile [27]. The patterns of innervation and gene expression remain very similar to that of the competent larvae (compare Fig. 5 with Fig. 7, and Additional file 3: Supplementary Fig. 3 with Additional file 6: Supplementary Fig. 6), except that now there are RGW-lir neurons on the lower mouth lip (lml; Fig. 6g–h; Additional file 6: Supplementary Fig. 6e–f). At this stage, *soxC* is broadly expressed in the mouth, and *six3/6* and *nk2.1* are expressed in the dorsal part of the foregut. *Otx* is now expressed in the boundary between the foregut and the midgut (Fig. 7a–b, e–f, g–j), suggesting an additional role in the neural innervation of the foregut. Altogether, our findings indicate that significant changes in the neural architecture occur during metamorphosis, as the originally bilobed brain transforms into a ring and connects with the anterior part of the trunk, establishing the final nervous system architecture of the juvenile/adult.

The juvenile nervous system

After metamorphosis, the juvenile body subdivides into the head — with the fused prostomium and peristomium — and the trunk, further differentiating into three fused thoracic segments, seven abdominal segments, and the pygidium [27] (Fig. 8). The mouth is anterior, and the brain ring is positioned dorsal to the roof of the foregut [23]. The brain ring comprises 5HT-lir, FMRFamide-lir, and tubulin$^+$ roots, connected via lateral medullary cords around the foregut to the vnc [9, 12, 23]. The vnc has iterated 5HT-lir neurons in an otherwise continuous medullary cord with no discontinuities, as seen with *ChAt* expression [9, 12, 23]. Consistently, FVamide-lir, RYamide-lir, RGWamide-lir, and MIP-lir localise to the ring-shaped brain that connects to the vnc with lateral medullary cords at the ciliated thoracic segments

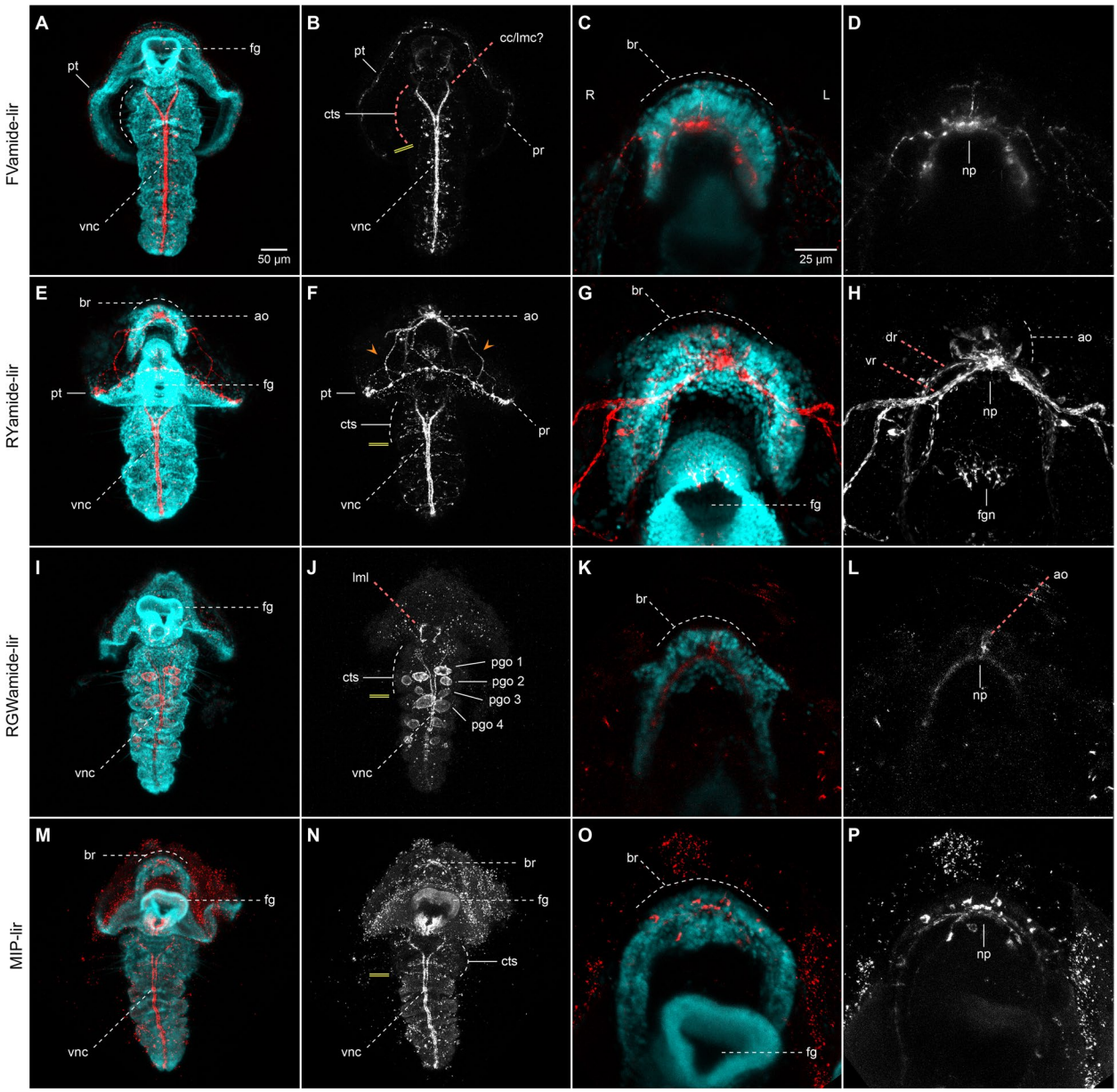

Fig. 6 Neuropeptide-lir elements during metamorphosis. CLSM images of DAPI (cyan) and neuropeptide$^+$ (red or white) elements during metamorphosis (~ 3–4 wpf). Ventral views, with anterior to the top. **c**–**d**, **g**–**h**, **k**–**l**, **o**–**p** are close ups of the apical organ and brain in the same view as the respective larger image in **a**–**b**, **e**–**f**, **i**–**j**, **m**–**n**. **a**–**b**, **e**–**f**, **i**–**j**, **m**–**n** The brain connects with the ventral nerve cord (vnc), via circumesophageal connectives (lateral medullary cords [22] at the trunk thorax, made out of three ciliated thoracis segments (cts). Iterated **a**–**b** FVamide-lir, **e**–**f** RYamide-lir and **m**–**n** MIP-lir neurons and transverse lateral nerves are present in the segments of the trunk. **i–j** RWG labels the parapodial glandular organs (pgos). Double yellow line marks the division between thoracic and abdominal segments. ao: apical organ; ar: apical nerve ring; br: brain; cc: circumesophageal connectives; cts: ciliated thoracic segments; dr: dorsal root; fg: foregut; fgn: foregut nerve; lmc: lateral medullary cords; lml: lower mouth lip; np: brain neuropil; pgo: parapodial glandular organ 1–4; pr: prototrochal ring; pt: prototroch; vnc: ventral nerve cord; vr: ventral root

(Fig. 8). FVamide-lir and RYamide-lir clusters of neurons (Fig. 8a–d) and FVamide-lir, RYamide-lir, and tubulin$^+$ peripheral nerves (Additional file 7: Supplementary Fig. 7c–d) occur in the anterior part of each segment, with one tubulin$^+$ pair of lateral nerves more prominent in each of the segments (ln; Additional file 7: Supplementary Fig. 7c–d). Tubulin$^+$ longitudinal nerve tracts run alongside the median vnc (cyan arrows; Additional file 7: Supplementary Fig. 7c) and ventrolaterally (magenta arrows; Additional file 7: Supplementary Fig. 7c–d).

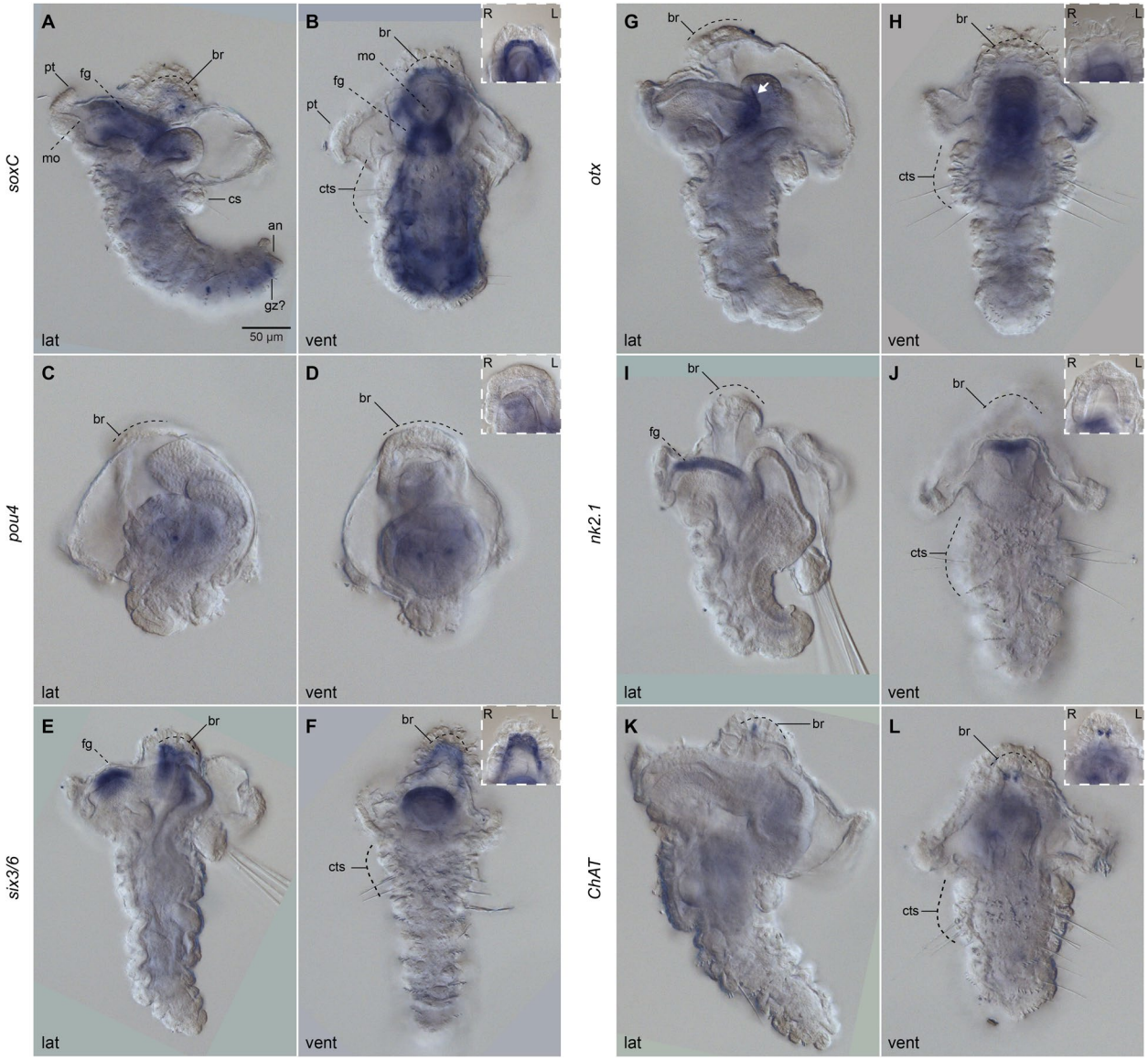

Fig. 7 Neural development during metamorphosis. DIC images showing expression of *soxC*, *pou4*, *six3/6*, *otx*, *nk2.1* and *ChAt*. **a**, **c**, **e**, **g**, **i** Lateral views; **b**, **d**, **f**, **h**, **j**, ventral views. Insets are close ups focusing on the brain of the corresponding larger images. **a**–**b** *soxC*, **e**–**f** *six3/6* and **k**–**l** *ChAT* are expressed in the brain (br). **a**–**b** *soxC* is expressed throughout the trunk, the foregut (fg), and in the putative growth zone (gz). **e**–**f** *six3/6* and **i**–**j** *nk2.1* are expressed on the dorsal side of the foregut, while **g**–**h** *otx* is expressed in the boundary between foregut and midgut (white arrow). an: anus; br: brain; cc: circumesophageal connectives; cts: ciliated thoracic segments; dr: dorsal root; fg: foregut; fgn: foregut nerve; lmc: lateral medullary cords; lml: lower mouth lip; np: brain neuropil; pgo: parapodial glandular organ 1–4; pr: prototrochal ring; pt: prototroch; vnc: ventral nerve cord; vr: ventral root

RGWamide-lir and MIP-lir nerves are also present in the mouth opening (Fig. 8e–h). At this stage, *six3/6* and weakly *soxC* are expressed in the brain (Additional file 8: Supplementary Fig. 8a–f). The latter is also expressed in the foregut and the putative posterior growth zone (gz), just before the pygidium (Additional file 8: Supplementary Fig. 8a–c). Therefore, the definitive brain is primarily formed in the juvenile. However, as described below, the vnc neuroarchitecture is more elaborated at this stage than in the adult [12, 22].

The anterior adult neural structures

The head of the adult *O. fusiformis* includes a crown of tentacles formed from the fused prostomium and peristomium and a pair of ventrolateral eyes [22, 37] (Fig. 9a). The FVamide-lir, RYamide-lir, RGWamide-lir, and

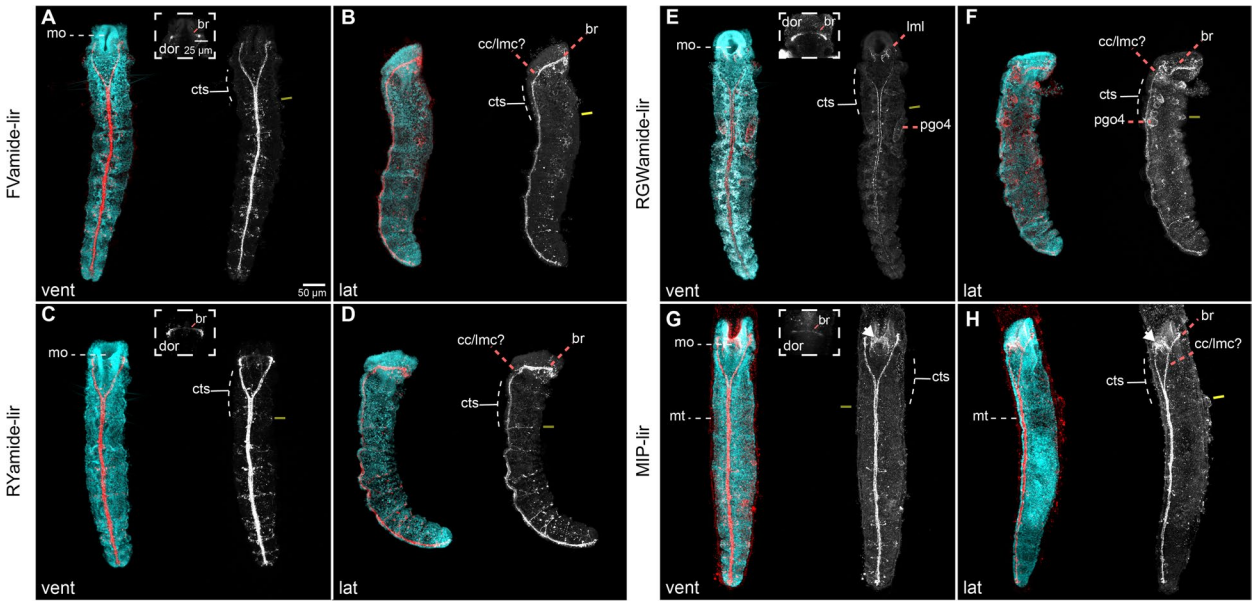

Fig. 8 Neuropeptide-lir elements in the juveniles. CLSM images of DAPI (cyan) and neuropeptide-lir (red or white) elements in juveniles (> 4 wpf). **a**, **c**, **e**, **g** Ventral views; **b**, **d**, **f**, **h** lateral views, with anterior to the top. The brain connects with the ventral nerve cord (vnc), via circumesophageal connectives (lateral medullary cords [22] at the trunk thorax, made out of three ciliated thoracic segments (cts). Iterated **a**–**b** FVamide-lir, **c**–**d** RYamide-lir and **g**–**h** MIP-lir neurons and lateral transverse nerves (ln) are present in the segments of the trunk. **e**–**f** RWG labels the parapodial glandular organs (pgos). Double yellow line marks the division between thoracic and abdominal segments. br: brain; cc: circumesophageal connectives; cts: ciliated thoracic segments; lmc: lateral medullary cords; lml: lower mouth lip; mo: mouth; mt: mucous tube; pgo: parapodial glandular organ 1–4; vnc: ventral nerve cord

MIP-lir nervous system is preserved throughout the ring-shaped brain, medullary cords, and vnc as seen in the juvenile (Fig. 9; Additional file 9: Supplementary Fig. 9). The neuropile of the brain is composed of parallel bundles of axons transverse to the lateral medullary cords, with FVamide-lir, RYamide-lir, RGWamide-lir, and MIP-lir neurons on the anterior and posterior edges (Fig. 9b, d, f, h; Additional file 9: Supplementary Fig. 9c, f, i, l). The FVamide-lir and RYamide-lir neuropil is wider than the RGWamide-lir and MIP-lir. The RYamide-lir neurons of the neuropil partially distinguish the dorsal and ventral roots of the brain as two concentrated bundles of neurites parallel to one another, separated by a less dense portion of neurites (Additional file 9: Supplementary Fig. 9f), suggesting some level of compartmentalisation in the apparently simple ring-shaped brain of this annelid. Finally, there are FVamide-lir, RYamide-lir, RGWamide-lir, and MIP-lir longitudinal head nerves lateral to the brain (Additional file 9: Supplementary Fig. 9b, f, j, n) that project anteriorly to the tentacles [22], and posteriorly into the trunk.

In addition to the brain, FVamide-lir, RYamide-lir, RGWamide-lir, and MIP-lir somata are present throughout the head tentacles (Fig. 9a–h) and surrounding the eyes (Fig. 9a, c, e, g; Additional file 9: Supplementary Fig. 9a, d, g, j). In these visual organs, a posterolateral cluster of neurons exhibits primarily FVamide-lir but also some RYamide-lir and MIP-lir signal, while RYamide-lir dominates in a second anterior cluster, which also shows some FVamide-lir and MIP-lir (Fig. 9a, c, g; Additional file 9: Supplementary Fig. 9a, d, j). However, this immunoreactivity is not part of the eye structure (21). A dorsal nerve cord composed of FVamide-lir, RYamide-lir, RGWamide-lir, and MIP-lir neurites and somata extends across the dorsal side of the body (Additional file 9: Supplementary Fig. 9b, e, h, k). Some of these immunoreactivity patterns in the head support previously observed 5HT-lir and FMRFamide-lir clusters in other oweniids [43, 44]. Our findings support that the adult brain and trunk nervous system are compartmentalised during the gradual reorganisation of the nervous system from larval and juvenile stages.

Discussion

This study characterises the ontogeny of the nervous system in *O. fusiformis* from larvae to adulthood using a set of conserved cross-species antibodies and gene expression. The morphological landmarks presented here will serve as a foundation to understand larval development, metamorphosis, and post-larval morphogenesis in an annelid occupying a critical phylogenetic position, which will help to infer ancestral characters to Annelida and

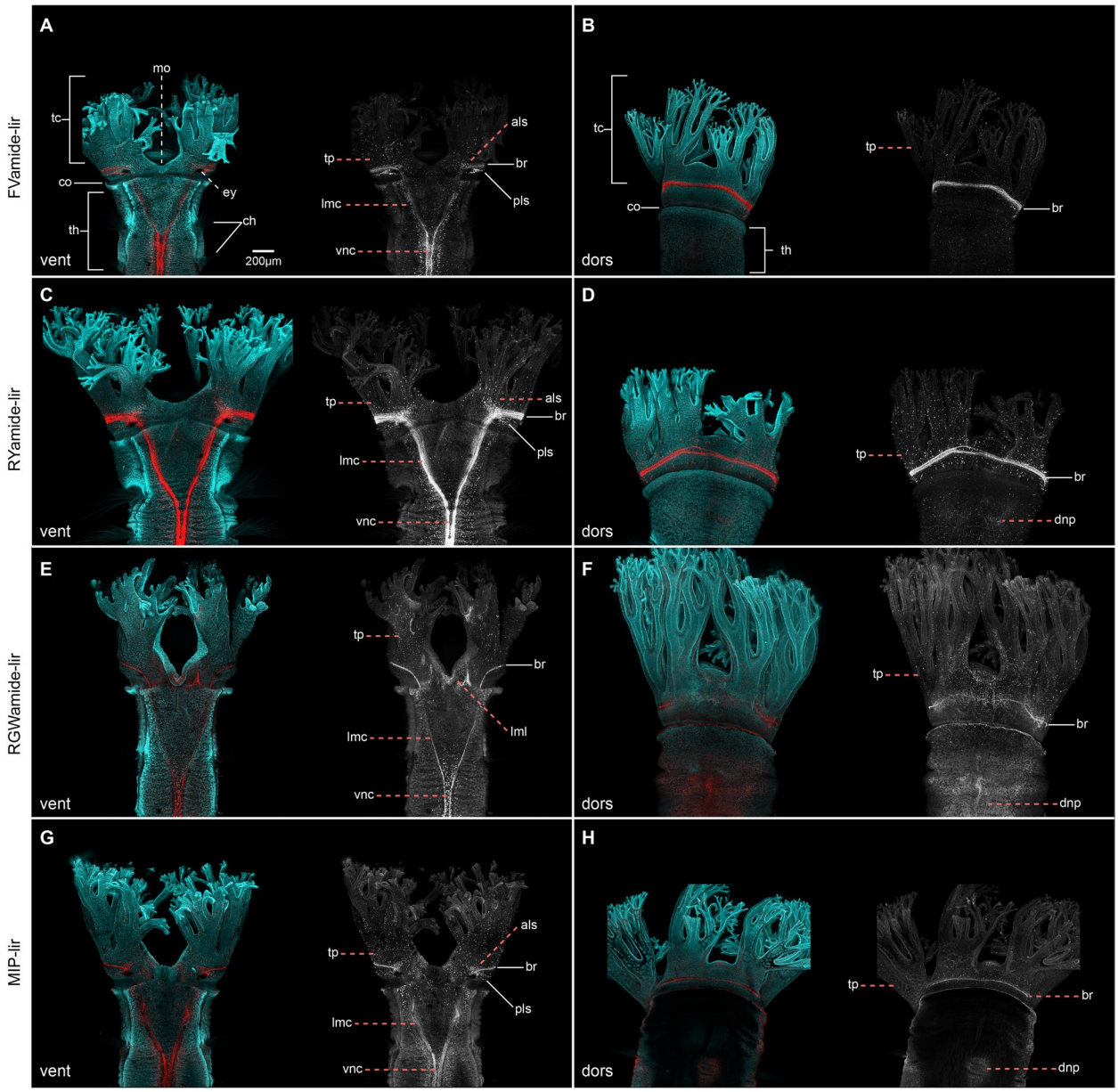

Fig. 9 Neuropeptide-lir elements in the head of adults. CLSM images of DAPI (cyan) and neuropeptide-lir (red or white) elements. **a**, **c**, **e**, **g** ventral views; **b**, **d**, **f**, **h** dorsal views. **a**, **c**, **e**, **g** The FVamide-lir, RYamide-lir, RGWamide-lir and MIP-lir brain ring (br) is connected via lateral medullary cords (lmc) to the ventral nerve cord (vnc) at the position of the thorax (th). Each tentacle of the head contains a basiepidermal nerve plexus (tp), which projects from the brain. **b**, **d**, **f**, **h** Posterior to the head there is a dorsal nerve plexus (dnp). Surrounding each eye are clusters of somata oriented in an anterior-lateral (als) and posterior-lateral position (pls) position, showing FVamide-lir, RYamide-lir, and MIP-lir. als: anterio-lateral somata; br: brain; ch: chaetae; co: collar; dorsal nerve plexus: dnp; ey: eye; lmc: lateral medullary cord; lml: lower mouth lip; pls: posterior-lateral somata; tc: tentacle crown; th: thorax; tp: tentacle plexus; vnc: ventral nerve cord

animals in general (Fig. 10; Additional file 10: Supplementary Table 1).

The nervous system in the early larva

The mitraria larva largely derives from anterior/head tissues [29], and posterior territories are limited to a ventral epithelial invagination that will form the juvenile rudiment trunk [24, 27] and a small dorsal posterior tissue that includes the anus and chaetal sac [34]. The larval neural system — composed of the apical organ and apical tuft connected to a prototroch ring — starts developing by 13 h post fertilisation (hpf) and connects to the

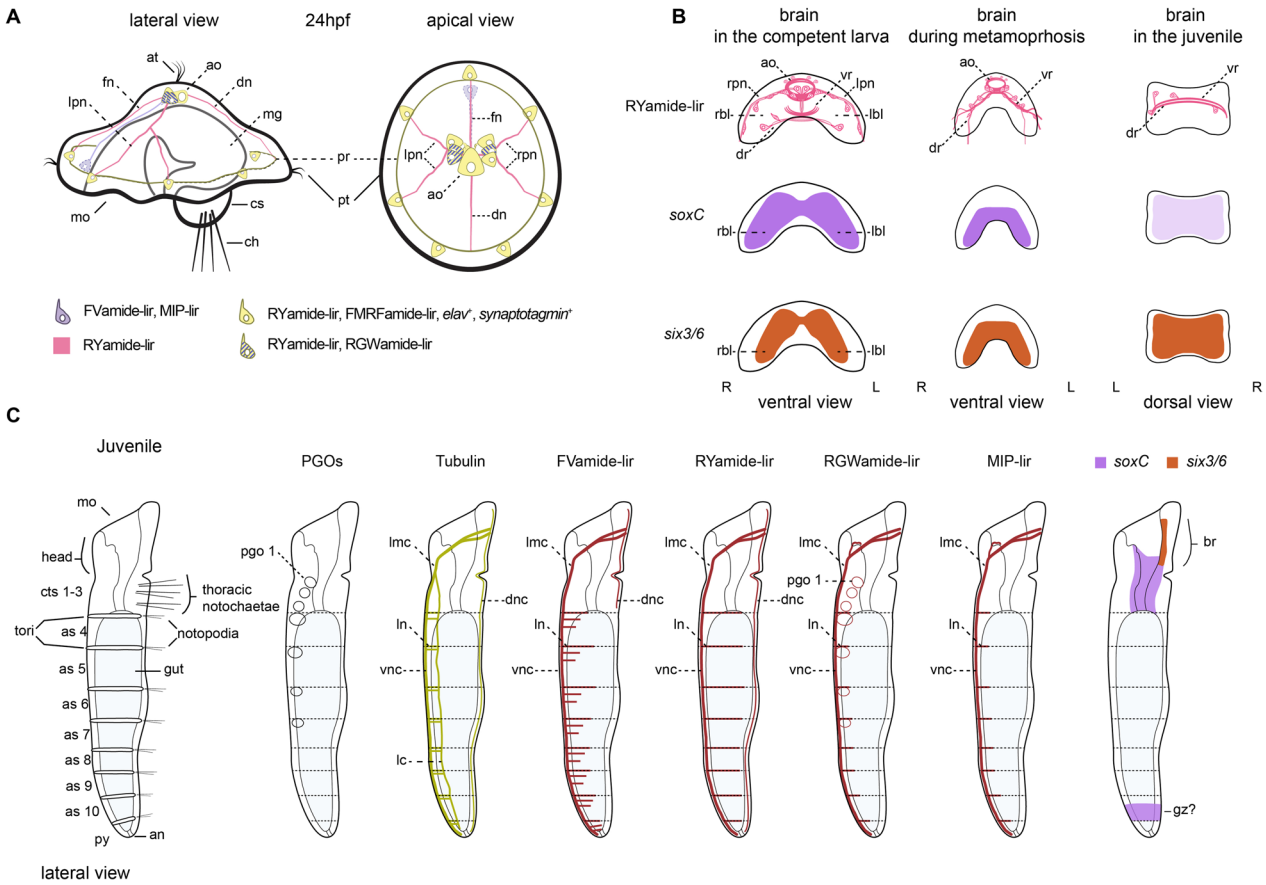

Fig. 10 Diagram of neural development in *O. fusiformis*. **a** At 24 hpf there is an FVamide-lir, RYamide-lir, RGWamide-lir, MIP-lir and FMRFamide-lir apical organ with *elav*$^+$ and *synaptotagmin*$^+$ cells that connect to the prototroch ring [24]. **b** The brain goes from a bilobed structure in the pre-competent larvae, to a nerve ring in the juvenile **c** Pattern of immunoreactivity and *soxC* and *six3/6* expression in the juvenile. ao: apical organ; as: abdominal segment; at: apical tuft; br: brain; ch: chaetae; cs: chaetal sac; cts: ciliated thoracic segment; dn: dorsal nerve; dnc: dorsal nerve cord; dr: dorsal root; fn: frontarl nerve; gz: growth zone; lc: lateral cord; lmc: lateral medullary cords; lpn: left peripheral nerve; mg: midgut; pgo: parapodial glandular organ; pr: prototroch ring; pt: prototroch; rbl: right brain lobe; rpn: right peripheral nerve; vr: ventral root

FMRFamide-lir prototroch ring by 24 hpf. The nervous system also includes seven FMRFamide-lir, *elav*$^+$ and *synaptotagmin*$^+$ neurons in the prototroch [24]. Our findings support this early neural architecture of the mitraria larva and reveal further complexity and refinement, particularly in the apical organ and its connections to the prototrochal neural ring. As in *P. dumerilii*, the apical organ contains FVamide-lir, RYamide-lir, RGWamide-lir, and MIP-lir neurons in *O. fusiformis*, some of which are monociliated. All these neuropeptides form a neurosecretory centre that regulates the swimming behaviour of the larvae of *P. dumerilii* [31, 32, 45, 46] (Additional file 10: Supplementary Table 1). They are also present in the anterior neural systems of other annelid and spiralian larvae, as in *C. teleta*, and even directly developing species [30–32, 35] (Additional file 10: Supplementary Table 1). In *O. fusiformis*, the apical organ connects frontally, bilaterally, and dorsally to the prototroch (Fig. 10a). The monociliary nature of the neuropeptide-lir neurons in the apical organ and the seven RYamide-lir neurons in the prototroch indicate they might have a sensory function (Fig. 10a). They presumably integrate stimuli from the apical organ and the prototroch to control the shape of the episphere and the ciliary beating, thus influencing the locomotion and behaviour of the larva, without the need for excess neural wiring as hypothesised for larvae with monociliated cells [47].

The spatial patterns of immunoreactivity show notable similarities between *O. fusiformis* and *P. dumerilii*. In both larvae, RY [31], FV [30, 31, 48, 49], and MIP [32, 48–50] occur in ciliated sensory neurons. However, RY and RGW are expressed in interneurons that communicate to the synaptic nervous system in *P. dumerilii* [48, 49, 51, 52] (Additional file 10: Supplementary Table 1). Future studies of the connectome in *O. fusiformis* could clarify if this is true for *O. fusiformis*. Nonetheless, the presence

of diverse neuropeptide sensory neurons, together with the deployment of staggered apical expression domains of transcription factors like *foxQ2*, *six3/6* and *otx* [11, 33, 53] (Additional file 10: Supplementary Table 1), support the evolutionary conservation of the apical region between annelids and spiralians and reveal anatomical traits of the anterior neural system of the ancestral "head swimming larva" of annelids.

From a bilobed larval brain to an adult ring-shaped brain

With growth, the neural features present in the early larva become more elaborated [23, 24], and the adult nervous system develops, first with the condensation of nuclei that form the brain (Fig. 10b) and later, with the patterning, elongation and subsequent evagination of the trunk. Nuclear staining, the expression of the anterior marker genes *ChAt*, *nk2.1*, *otx*, *pou4*, and *six3/6* [9, 33, 34], and neuropeptide immunoreactivity reveal that the pre-metamorphic larva has a bilobed brain (Fig. 10b). This is consistent with classic morphological descriptions [27] and similar to the larvae of other "early branching" [54, 55] and more divergent annelids [15, 16, 56]. The brain sits underneath a prominent neuropeptide-rich apical organ (Fig. 10b), which comprises an apical ring and several neurons surrounding the monociliated apical tuft. Anterior and posterior FMRFamide-lir and 5HT-lir [23] and RYamide-lir axonal roots form a neuropil underneath the brain referred to as ventral and dorsal roots in other annelids, respectively [14, 41]. Remarkably, this organisation changes with metamorphosis, as the bilobed brain forms a continuous *soxC*+and *six3/6*+band that compresses anteroposteriorly, bringing the dorsoventral roots closer to each other (Fig. 10b). This results in the fusion of the brain lobes and roots into a double ring that forms the brain in the juvenile [23] and adult [22]. While our data support a reorganisation of the brain from larval to adult stages [22, 25, 26], we were unable to determine the fate of the larval apical organ, and it remains unclear whether it integrates into the juvenile brain or is resorbed during metamorphosis with the apical tuft and prototroch.

From metamorphosis onwards, the roots of the brain neuropil connect with lateral medullary cords, ending into a medullary non-ganglionated, medially-condensed vnc in the trunk [12, 22]. The presence of bundles of axons with distinct neuropeptide immunoreactivity in the adult brain ring suggests an unexpected level of compartmentalisation in this previously regarded "simple" brain [22] that might indicate the retention of the anterior and posterior roots ("ventral" and "dorsal", respectively, according to traditional anatomical descriptions [14, 41]) seen in the larval and metamorphic stages in adult stages. This would challenge hypotheses based on the analysis of other oweniids that their ring-shaped brain is homologous to the dorsal (posterior) root neuropil of other annelids [43, 44]. Despite its presumable compartmentalisation, there are no distinct ganglionic centres in the adult brain of *O. fusiformis*, unlike in more active annelids that exhibit structures like the mushroom bodies and nuchal organs [57, 58]. Therefore, the brains of *O. fusiformis* and other representatives of the "early branching" clades gradually reorganise their morphology while retaining neuronal diversity during metamorphosis to form a continuous medullary cord with the vnc, perhaps associated with a transition to a more sedentary, tube-dwelling lifestyle as adults.

From a juvenile rudiment to the trunk nervous system

The trunk of oweniids forms as an invagination of the ventral epithelium of the larva [27, 28] with the deployment of conserved anterior-posterior and trunk-patterning programmes like the *hox* genes [29]. While neurogenesis, as revealed by the expression of *elav, synaptotagmin* [24], and *soxC* (this study), is predominant in the apical organ and brain region in the early larva, it mainly occurs in the developing trunk before metamorphosis. As in other annelids [9, 12], the trunk nervous system develops as a paired medially-condensed vnc, but, most notably, it also includes a single dorsal nerve cord connected to the ventral one by segmentally iterated lateral nerves (Additional file 10: Supplementary Table 1). During metamorphosis, additional ventrolateral longitudinal cords form, giving the trunk nervous system an orthogonal appearance that has been hypothesised to be the ancestral pattern for annelids [59] and other spiralians, such as flatworms and nemerteans [60, 61]. A ganglionated ladder-like vnc thus likely evolved independently multiple times in annelids and other animals [9, 12]. As the juvenile worm matures into adulthood, more neurons appear along the vnc, resulting in a continuous medullary cord with no apparent breaks [12, 22, 43]. However, the lack of segmented ganglia in the vnc of *O. fusiformis* does not exclude the presence of clusters of 5HT-lir [9, 12, 23] and FVamide-lir, RYamide-lir and MIP-lir (this study) neurons in each segment. Parapodial glandular organs (PGOs) [42] develop in each of the first seven segments [27] and show RGWamide-lir, which combined with the cilia of the thoracic segments and the neuropeptide-lir and tubulin^{+} lateral nerves of the abdominal segments, define positional landmarks along the anterior-posterior axis that would aid in the study of trunk formation in *O. fusiformis* (Fig. 10c). Concurrent with the maturation of the brain and trunk nervous system, the immunoreactivity in the larval foregut and definitive oesophagus changes. In *O. fusiformis*, the foregut of the competent larvae is innervated by 5HT-lir and FMRFamide-lir [23,

24], and FVamide-lir and RYamide-lir neurons and axons (this study); and by 5HT-lir [23] and RGWamide-lir and MIP-lir (this study) in the juvenile stage. FMRFamide-lir neurons and axons innervate the enteric nervous system of juvenile annelids like *C. teleta* [15]. At the same time, MIP is also present in the stomatogastric nervous system in dinophilids [35], and it plays a role in the feeding behaviour of *P. dumerilii* larva [50], suggesting a conserved neuropeptide-mediated control of feeding in annelids.

Conclusions

Our study describes the transition of the nervous system from the early larva to the adult stage in the annelid *O. fusiformis*, a representative of Oweniidae and the sister lineage to all remaining annelids. The initial larval neural system comprises an apical organ connected to a prototrochal ring and the chaetal sac through several neurites. Soon, a bilobed brain forms underneath the apical organ, connecting with other larval tissues and the developing juvenile trunk in its anterior part. During metamorphosis, the lobes, and the ventral and dorsal roots fuse to form a ring-shaped brain, following a similar trend of reorganisation of the neural architecture as in other "early branching" annelids like magelonids and chaetopterids [22, 25, 26]. However, our findings indicate that the larval and adult nervous systems are not as simple as previously thought in *O. fusiformis* and retain similarities with more deeply nested annelids, particularly at the larval stages. Future studies of the detailed connectome of the mitraria larva will help to understand how these anatomical similarities translate into conservation of behaviours and physiological functions, illuminating how neuropeptidergic systems might have contributed to the evolution of biphasic life cycles.

Abbreviations

als	Anterior-lateral somata
an	Anus
ao	Apical organ
ar	Apical nerve ring
at	Apical tuft
br	Brain
CLSM	Confocal laser scanning microscopy
cc	Circumesophageal connective
chn	Chaetal sac nerve
co	Collar
cs	Chaetal sac
cts	Ciliated thoracic segment
dn	Dorsal nerve
dnc	Dorsal nerve cord
dr	Dorsal root
fg	Foregut
fgn	Foregut nerve
fn	Frontal nerve
gz	Growth zone
jr	Juvenile rudiment
lc	Lateral cord
lmc	Lateral medullary cord
lml	Lower mouth lip
ln	Lateral transverse nerve
lpn	Left peripheral nerve
mg	Midgut
MIP	Myoinhibitory peptide
mo	Mouth
mt	Mucous tube
ne	Neurite
np	Brain neuropil
nph	Nephridia
pgo	Parapodial glandular organ
pls	Posterior-lateral somata
pr	Prototrochal ring
pt	Prototroch
so	Somata
rg	Refringet globule
rpn	Right peripheral nerve
tc	Tentacle crown
th	Thorax
tp	Tentacle plexus
vnc	Ventral nerve cord
vr	Ventral root

Supplementary Information

The online version contains supplementary material available at https://doi.org/10.1186/s13064-024-00180-8.

Additional file 1: Supplementary Fig. 1. Alignment of the neuropeptide precursors *P. dumerilii* [30–32], *C. teleta* [62] and *Owenia fusiformis* [29]. Representative mature peptides and conserved dipeptides are highlighted in red and bold, respectively.

Additional file 2: Supplementary Fig. 2. MIP-lir elements in the 24hpf mitraria. MIP-lir cells include several cells as part of the apical organ (ao) and one cell anterior to the foregut (white arrow), including a MIP-lir frontal nerve (fn). Inset in b is a close up of the apical organ (ao) in the same view as the larger image. ao: apical organ; at: apical tuft; cs: chaetal sac; fn: frontal nerve; mo: mouth.

Additional file 3: Supplementary Fig. 3. Neuropeptide-lir elements in the competent larvae. CLSM images of DAPI (cyan), acetylated tubulin (yellow) and neuropeptide-lir (red or white) elements in the competent larvae (~ 3 wpf). Lateral views, with anterior to the left. c, f, i, l are close ups of the juvenile rudiment in the same view as the respective larger image in b, e, h, k. a–c FVamide-lir cells and MIP-lir cells in the apical organ connect via FVamide-lir and MIP-lir circumesophageal connectives (cc) to the ventral nerve cord (vnc) of the juvenile trunk rudiment (jr), and via a–b FVamide-lir, d–e RYamide-lir and j–k MIP-lir frontal (fn), dorsal (dn) and peripheral nerves (closed orange arrow heads) to the a–c FVamide-lir, d–f RYamide-lir and j–l MIP-lir prototrochal ring (pr). See also Fig. 2. d–f RYamide-lir and j–l MIP-lir peripheral nerves also branch out to the chaetal nerve (chn) (open pink arrowheads). The foregut is innervated by a–c FVamide-lir and d–f RYamide-lir cells and neurites. By this stage the juvenile rudiment has a vnc and a a–c FVamide-lir and d–f RYamide-lir dorsal nerve cord (dnc). g–i RGWamide-lir cells are only present in the apical organ. j–l MIP-lir is present in the anterior part of the foregut (white arrow). an: anus; ao: apical organ; at: apical tuft; br: brain; cc: circumesophageal connectives; chn: chaetal sac nerve; cs: chaetal sac; dn: dorsal nerve; dnc: dorsal nerve cord; fg: foregut; fgn: foregut nerve; fn: frontal nerve; jr: juvenile rudiment; mg: midgut; mo: mouth; pr: prototrochal ring; pt: prototroch; vnc: ventral nerve cord.

Additional file 4: Supplementary Fig. 4. Tubulin$^+$ elements in the competent. CLSM images of beta-tubulin (a–e) and alpha-acetylated tubulin (f–j) in the competent larvae (~ 3 wpf). a–c, g–h apical views; d–e, i–j, lateral views; f ventral view. a–c, g–h the apical organ (ao), associated with an apical tuft (at) and apical nerve ring (ar) is positioned above the brain (br). Ventral (vr) and dorsal (dr) roots c, h make the neuropil of the brain, that connects with the d circumesophageal connectives (cc), and ultimately with the ventral nerve cord (vnc) d–e. f, i–j Tubulin$^+$ peripheral

nerves (fn, dn, and orange arrowheads) connect the apical organ with the prototroch ring (pr). ao: apical organ; an: anus; ar: apical nerve ring; at: apical tuft; br: brain; cb: chaetoblast; cc: circumesophageal connectives; chn: chaetal sac nerve; cs: chaetal sac; dn: dorsal nerve; dnc: dorsal nerve cord; dr: dorsal root; fg: foregut; fgn: foregut nerve; fn: frontal nerve; jr: juvenile rudiment; mg: midgut; mo: mouth; nph: nephridia; pr: prototrochal ring; pt: prototroch; vnc: ventral nerve cord; vr: ventral root.

Additional file 5: Supplementary Fig. 5. SoxC orthology and early mRNA expression. a Maximum likelihood orthology assignments of *soxC*. b DIC images showing expression of *soxC* during gastrulation (9hpf) and early mitraria (24hpf). Asterisks mark the animal/apical pole an: anus; bp: blastopore; cs: chaetal sac; fg: foregut; mo: mouth; pt: prototroch.

Additional file 6: Supplementary Fig. 6. Neuropeptide-lir elements during metamorphosis. CLSM images of DAPI (cyan) and neuropeptide-lir (red or white) elements during metamorphosis (~ 3 4pf). Lateral views, with anterior to the top. a–hThe brain connects with the ventral nerve cord (vnc), via circumesophageal connectives (lateral medullary cords [22] at the trunk thorax, made out of three ciliated thoracis segments (cts). The foregut (fg) has b FVamide-lir, f RYamide-lir and h MIP-lir neurons and cells. e–f RWGamide labels the parapodial glandular organs (pgos), and the lower mouth lip (lml). Double yellow line marks the division between thoracic and abdominal segments. ao: apical organ; an: anus; br: brain; cc: circumesophageal connectives; cts: ciliated thoracic segments; dn: dorsal nerve; dr: dorsal root; fg: foregut; fgn: foregut nerve; lmc: lateral medullary cords; lml: lower mouth lip; np: brain neuropil; pgo: parapodial glandular organ 1–4; pr: prototrochal ring; pt: prototroch; vnc: ventral nerve cord; vr: ventral root.

Additional file 7: Supplementary Fig. 7. Tubulin^{+} elements during metamorphosis and juvenile. CLSM images of acetylated tubulin. a–b Larvae undergoing metamorphosis. c–d > 4 wfp juvenile. a–b Tub^{+} peripheral nerves (orange arrowheads) in the remaining episphere of the larva keep connecting the brain to the prototrochal ring (pr). a–d The brain connects with the ventral nerve cord (vnc), via circumesophageal connectives (lateral medullary cords [22] at the trunk thorax, made out of three ciliated thoracis segments (cts). The vnc is composed of two robust longintudinal tracts, and two more lateral tracts (magenta arrows). On the anterior border of each segment, there is a pair of lateral transverse nerves (ln) that connect to lateral ventral-lateral longitudinal cords (magenta arrows). Double yellow line marks the division between thoracic and abdominal segments. ao: apical organ; br: brain; cc: circumesophageal connectives; cts: ciliated thoracic segments; dr: dorsal root; fn: frontarl nerve; lmc: lateral medullary cords; ln: lateral transverse nerves; nph: nephridia; pr: prototrochal ring; pt: prototroch; vnc: ventral nerve cord; vr: ventral root.

Additional file 8: Supplementary Fig. 8. Neural development in juveniles. DIC images showing expression of *soxC*, *pou4*, *six3/6* and *otx*. a, d, g, j Lateral views; b, e, h, k ventral views; c, f, i, l dorsal views. a–c*soxC* and d–f *six3/6* are expressed in the brain (br). g–i *pou 4* and j–l *otx* have no longer any neural expression. a–c*soxC* is expressed in the foregut (fg), and in the putative growth zone (gz). br: brain; fg: foregut; gz: growth zone; mo: mouth.

Additional file 9: Supplementary Fig. 9. Neuropeptide-lir elements in the adults. CLSM images of neuropeptide-lir close ups of images in Fig. 9. a–b, e–f, i–j, m–n ventral views; c–d, g–h, k–l, o–p dorsal views. a, e, i, m Views of the eye showing FVamide-lir, RYamide-lir and MIP-lir, antero-lateral (als) and postero-lateral (pls) somata. b, f, j, n Lateral head neurites (lhn) extend toward the tentacles and the trunk. c, g, k, o Longitudinal dorsal nerve cord (dnc). d, h, l, p Brain ring with associated neurites (ne) and somata (so). als: anterior-lateral somata; br: brain; dnc: dorsal nerve cord; ey: eye; lhn: lateral head neurites; lmc: lateral medullary cord; ne: neurite; pls: posterior-lateral somata; so: somata; tp: tentacle plexus.

Additional file 10: Supplementary Table 1. Immunoreactivity of neuropeptide and gene expression during the neurogenesis of several annelid species.

Acknowledgements
We thank all members of the Martín-Durán lab for their support. We thank Océane Seudre for amplifying and synthesising the *soxC* probe and Paul Kalke for recommendations regarding immunostaining of the adult heads. We also thank the Station Biologique de Roscoff for their help with collections and animal supplies.

Authors' contributions
AMCB and JMMD designed the study. AMCB and RD performed all the immunostainings and fluorescence imaging. AMCB performed the expression analyses and imaging of gene expression. EAW and GJ contributed with reagents and sequencing data. AMCB, RD and JMMD built the figures. AMCB drafted the manuscript. All authors contributed to data interpretation and manuscript writing.

Funding
This study was funded by the Company of Biologists (Travel fellowship grant JEBTF2205748) to AMCB and the European Research Council (Starting Grant, Action number 801669) to JMMD.

Availability of data and materials
No datasets were generated or analysed during the current study.

Declarations

Ethics approval and consent to participate
Not applicable.

Consent for publication
Not applicable.

Competing interests
The authors declare no competing interests.

Received: 14 November 2023 Accepted: 2 February 2024
Published online: 21 February 2024

References

1. Jékely G, Keijzer F, Godfrey-Smith P. An option space for early neural evolution. Philos Trans R Soc Lond B Biol Sci. 2015;370:1684.
2. Bullock TH, Horridge GA. Structure and function in the Nervous systems of invertebrates. San Francisco: W. H. Freeman and Company; 1965. p. 1719.
3. Martín-Durán JM, Hejnol A. A developmental perspective on the evolution of the nervous system. Dev Biol. 2021;475:181–92.
4. Hejnol A, Lowe CJ. Embracing the comparative approach: how robust phylogenies and broader developmental sampling impacts the understanding of nervous system evolution. Philos Trans R Soc Lond B Biol Sci. 2015;370(1684):20150045.
5. Northcutt RG. Evolution of centralized nervous systems: two schools of evolutionary thought. Proc Natl Acad Sci U S A. 2012;109(Suppl 1):10626–33.
6. Hartenstein V, Stollewerk A. The evolution of early neurogenesis. Dev Cell. 2015;32(4):390–407.
7. Arendt D, Urzainqui IQ, Vergara HM. The conserved core of the nereid brain: Circular CNS, apical nervous system and *lhx6-arx-dlx* neurons. Curr Opin Neurobiol. 2021;71:178–87.
8. Liang Y, Carrillo-Baltodano AM, Martín-Durán JM. Emerging trends in the study of spiralian larvae. Evol Dev. 2023:e12459
9. Martín-Durán JM, Pang K, Borve A, Le HS, Furu A, Cannon JT, et al. Convergent evolution of bilaterian nerve cords. Nature. 2018;553(7686):45–50.
10. Denes AS, Jékely G, Steinmetz PR, Raible F, Snyman H, Prud'homme B, et al. Molecular architecture of annelid nerve cord supports common origin of nervous system centralization in Bilateria. Cell. 2007;129(2):277–88.

11. Marlow H, Tosches MA, Tomer R, Steinmetz PR, Lauri A, Larsson T, et al. Larval body patterning and apical organs are conserved in animal evolution. BMC Biol. 2014;12(7):1–17.
12. Helm C, Beckers P, Bartolomaeus T, Drukewitz SH, Kourtesis I, Weigert A, et al. Convergent evolution of the ladder-like ventral nerve cord in Annelida. Front Zool. 2018;15:36.
13. Purschke G, Annelida. Basal groups and Pleistoannelida. In: Schmidt-Rhaesa A, Harzsch S, editors. Structure and evolution of Invertebrate Nervous systems. Oxford: Oxford University Press; 2016. pp. 254–312.
14. Orrhage L, Müller CHG. Morphology of the nervous system of Polychaeta (Annelida). Hydrobiologia. 2005;535/536:79–111.
15. Meyer NP, Carrillo-Baltodano A, Moore RE, Seaver EC. Nervous system development in lecithotrophic larval and juvenile stages of the annelid *Capitella teleta*. Front Zool. 2015;12:15.
16. Vopalensky P, Tosches MA, Achim K, Handberg-Thorsager M, Arendt D. From spiral cleavage to bilateral symmetry: the developmental cell lineage of the annelid brain. BMC Biol. 2019;17(1):81.
17. Kumar S, Tumu SC, Helm C, Hausen H. The development of early pioneer neurons in the annelid *Malacoceros fuliginosus*. BMC Evol Biol. 2020;20(1):117.
18. Sur A, Magie CR, Seaver EC, Meyer NP. Spatiotemporal regulation of nervous system development in the annelid *Capitella teleta*. EvoDevo. 2017;8:13.
19. McDougall C, Chen WC, Shimeld SM, Ferrier DE. The development of the larval nervous system, musculature and ciliary bands of *Pomatoceros Lamarckii* (Annelida): heterochrony in polychaetes. Front Zool. 2006;3: 16.
20. Starunov VV, Voronezhskaya EE, Nezlin LP. Development of the nervous system in *Platynereis dumerilii* (Nereididae, Annelida). Front Zool. 2017;14:27.
21. Purschke G, Vodopyanov S, Baller A, von Palubitzki T, Bartolomaeus T, Beckers P. Ultrastructure of cerebral eyes in Oweniidae and Chaetopteridae (Annelida) - implications for the evolution of eyes in Annelida. Zoological Lett. 2022;8(1):3.
22. Beckers P, Helm C, Purschke G, Worsaae K, Hutchings P, Bartolomaeus T. The central nervous system of Oweniidae (Annelida) and its implications for the structure of the ancestral annelid brain. Front Zool. 2019;16:6.
23. Helm C, Vocking O, Kourtesis I, Hausen H. *Owenia fusiformis* - a basally branching annelid suitable for studying ancestral features of annelid neural development. BMC Evol Biol. 2016;16(1):129.
24. Carrillo-Baltodano AM, Seudre O, Guynes K, Martín-Durán JM. Early embryogenesis and organogenesis in the annelid *Owenia fusiformis*. EvoDevo. 2021;12(1):5.
25. Beckers P, Helm C, Bartolomaeus T. The anatomy and development of the nervous system in Magelonidae (Annelida) - insights into the evolution of the annelid brain. BMC Evol Biol. 2019;19(1):173.
26. Helm C, Schwarze G, Beckers P. Loss of complexity from larval towards adult nervous systems in Chaetopteridae (Chaetopteriformia, Annelida) unveils evolutionary patterns in Annelida. Organisms Divers Evol. 2022;22(3):631–47.
27. Wilson DP. On the mitraria larva of *Owenia fusiformis* Delle Chiaje. Philosophical Transcations Royal Soc B. 1932;221(474–482):231–334.
28. Smart TI, von Dassow G. Unusual development of the mitraria larva in the polychaete *Owenia collaris*. Biol Bull. 2009;217:253–68.
29. Martín-Zamora FM, Liang Y, Guynes K, Carrillo-Baltodano AM, Davies BE, Donnellan RD, et al. Annelid functional genomics reveal the origins of bilaterian life cycles. Nature. 2023;615(7950):105–10.
30. Conzelmann M, Jékely G. Antibodies against conserved amidated neuropeptide epitopes enrich the comparative neurobiology toolbox. EvoDevo. 2012;3: 23.
31. Conzelmann M, Offenburger SL, Asadulina A, Keller T, Munch TA, Jékely G. Neuropeptides regulate swimming depth of *Platynereis* larvae. Proc Natl Acad Sci U S A. 2011;108(46):E1174-1183.
32. Conzelmann M, Williams EA, Tunaru S, Randel N, Shahidi R, Asadulina A, et al. Conserved MIP receptor-ligand pair regulates *Platynereis* larval settlement. Proc Natl Acad Sci U S A. 2013;110(20):8224–9.
33. Martín-Durán JM, Passamaneck YJ, Martindale MQ, Hejnol A. The developmental basis for the recurrent evolution of deuterostomy and protostomy. Nat Ecol Evol. 2016;1(1): 5.
34. Seudre O, Carrillo-Baltodano AM, Liang Y, Martín-Durán JM. ERK1/2 is an ancestral organising signal in spiral cleavage. Nat Commun. 2022;13(1):2286.
35. Kerbl A, Conzelmann M, Jékely G, Worsaae K. High diversity in neuropeptide immunoreactivity patterns among three closely related species of Dinophilidae (Annelida). J Comp Neurol. 2017;525(17):3596–635.
36. Müller J, Bartolomaeus T, Tilic E. Formation and degeneration of scaled capillary notochaetae in *Owenia fusiformis* Delle Chiaje, 1844 (Oweniidae, Annelida). Zoomorphology. 2021;141(1):43–56.
37. Rouse GW, Pleijel F, Tilic E, Oweniidae Rioja. 1917. In: Rouse GW, Pleijel F, TIlic E, editors. Annelida. Oxford: Oxford University Press; 2022. p. 321-5.
38. Schnitzler C, Simmons DK, Pang K, Martindale MQ, Baxevanis AD. Expression of multiple *sox* genes through embryonic development in the ctenophore Mnemiopsis leidyi is spatially restricted to zones of cell proliferation. EvoDevo. 2014;5(15):1–17.
39. Price MN, Dehal PS, Arkin AP. FastTree 2–approximately maximum-likelihood trees for large alignments. PLoS ONE. 2010;5(3): e9490.
40. Rueden CT, Schindelin J, Hiner MC, DeZonia BE, Walter AE, Arena ET, et al. ImageJ2: ImageJ for the next generation of scientific image data. BMC Bioinformatics. 2017;18(1):529.
41. Müller MC. Polychaete nervous systems: Ground pattern and variations–cLS microscopy and the importance of novel characteristics in phylogenetic analysis. Integr Comp Biol. 2006;46(2):125–33.
42. Rimskaya-Korsakova N, Dyachuk V, Temereva E. Parapodial glandular organs in *Owenia borealis* (Annelida: Oweniidae) and their possible relationship with nephridia. J Exp Zool B Mol Dev Evol. 2020;334(2):88–99.
43. Rimskaya-Korsakova NN, Kristof A, Malakhov VV, Wanninger A. Neural architecture of *Galathowenia oculata* Zach, 1923 (Oweniidae, Annelida). Front Zool. 2016;13:5.
44. Temereva E, Rimskaya-Korsakova N, Dyachuk V. Detailed morphology of tentacular apparatus and central nervous system in *Owenia borealis* (Annelida, Oweniidae). Zoological Lett. 2021;7(1):15.
45. Veraszto C, Guhmann M, Jia H, Rajan VBV, Bezares-Calderón LA, Pineiro-Lopez C, et al. Ciliary and rhabdomeric photoreceptor-cell circuits form a spectral depth gauge in marine zooplankton. Elife. 2018;7:7.
46. Jokura K, Ueda N, Gühmann M, Yañez-Guerra LA, Słowiński P, Wedgwood KCA, et al. Nitric oxide feedback to ciliary photoreceptor cells gates a UV avoidance circuit. Elife. 2023;12(RP91258):1–52.
47. Jékely G. Origin and early evolution of neural circuits for the control of ciliary locomotion. Proc Biol Sci. 2011;278(1707):914–22.
48. Williams EA, Veraszto C, Jasek S, Conzelmann M, Shahidi R, Bauknecht P, et al. Synaptic and peptidergic connectome of a neurosecretory center in the annelid brain. Elife. 2017;6:6.
49. Williams EA, Jékely G. Neuronal cell types in the annelid *Platynereis dumerilii*. Curr Opin Neurobiol. 2019;56:106–16.
50. Williams EA, Conzelmann M, Jékely G. Myoinhibitory peptide regulates feeding in the marine annelid *Platynereis*. Front Zool. 2015;12(1):1.
51. Shahidi R, Williams EA, Conzelmann M, Asadulina A, Veraszto C, Jasek S, et al. A serial multiplex immunogold labeling method for identifying peptidergic neurons in connectomes. Elife. 2015;4:4.
52. Veraszto C, Ueda N, Bezares-Calderon LA, Panzera A, Williams EA, Shahidi R, et al. Ciliomotor circuitry underlying whole-body coordination of ciliary activity in the Platynereis larva. Elife. 2017;6:6.
53. Seudre O, Martín-Zamora FM, Rapisarda V, Luqman I, Carrillo-Baltodano AM, Martín-Durán JM. The fox gene repertoire in the annelid Owenia fusiformis reveals multiple expansions of the foxQ2 class in Spiralia. Genome Biol Evol. 2022;14(10):evac139.
54. Jackson DJ, Meyer NP, Seaver E, Pang K, McDougall C, Moy VN, et al. Developmental expression of *COE* across the Metazoa supports a conserved role in neuronal cell-type specification and mesodermal development. Dev Genes Evol. 2010;220(7–8):221–34.
55. Carrillo-Baltodano AM, Boyle MJ, Rice ME, Meyer NP. Developmental architecture of the nervous system in *Themiste lageniformis* (Sipuncula): new evidence from confocal laser scanning microscopy and gene expression. J Morphol. 2019;280(11):1628–50.
56. Meyer NP, Seaver EC. Neurogenesis in an annelid: characterization of brain neural precursors in the polychaete *Capitella* sp. I. Dev Biol. 2009;335(1):237–52.
57. Tomer R, Denes AS, Tessmar-Raible K, Arendt D. Profiling by image registration reveals common origin of annelid mushroom bodies and vertebrate pallium. Cell. 2010;142(5):800–9.
58. Heuer CM, Müller CHG, Todt C, Loesel R. Comparative neuroanatomy suggests repeated reduction of neuroarchitectural complexity in Annelida. Front Zool. 2010;7(13):1–21.

59. Purschke G. On the ground pattern of Annelida. Organisms Divers Evol. 2002;2(3):181–96.
60. Gustafsson MKS, Halton DW, Kreshchenko ND, Movsessian SO, Raikova OI, Reuter M, et al. Neuropeptides in flatworms. Peptides. 2002;23(11):2053–61.
61. Beckers P, Loesel R, Bartolomaeus T. The nervous systems of basally branching nemertea (Palaeonemertea). PLoS ONE. 2013;8(6): e66137.
62. Simakov O, Marletaz F, Cho SJ, Edsinger-Gonzales E, Havlak P, Hellsten U, et al. Insights into bilaterian evolution from three spiralian genomes. Nature. 2013;493(7433):526–31.

Publisher's Note